NASTRAN AS AN ANALYTICAL RESEARCH TOOL FOR COMPOSITE MECHANICS AND COMPOSITE STRUCTURES

C. C. Chamis, J. H. Sinclair, and T. L. Sullivan
Lewis Research Center

ABSTRACT

Selected examples are described in which NASTRAN is used as an analysis research tool for composite mechanics and for composite structural components. The examples were selected to illustrate the importance of using NASTRAN as an analysis tool in this rapidly advancing field. The results obtained demonstrate rather convincingly the versatility and effectiveness of NASTRAN in such applications.

INTRODUCTION

This paper describes selected examples in which NASTRAN was used as an analysis tool for composite mechanics and for composite structural components. Typical examples for composite mechanics include: stress analysis of the load transfer region of off-axis (with respect to fiber direction) composite specimens, the vibration response of specimens with defects, the effects of in-plane and out-of-plane (plane of specimen) eccentricities on test results, the stress variation in the load transfer region of thin composite tubular specimens, the stress distribution in the near and far field regions of a composite cantilevered plate subjected to a concentrated load, and the determination of the bending modulus in composite specimens with non-uniform thickness. The examples for composite structures include: stress analysis of composite blades for aircraft turbine engines, and stress and vibration analysis of a composite thin shell airfoil section.

The description of each example includes: the objective of the study, a brief background of its genesis, a schematic of the geometry, the finite element representation (number of grid points, number and type of elements, computer running times), typical results in graphical and/or tabular form, and comparisons with measured data when available.

OFF-AXIS COMPOSITE TENSILE SPECIMENS

The objective of using NASTRAN in this study was to predict the stress state near the end tabs and at mid length of off-axis composite specimens tested in tension. The results were subsequently used for comparisons with measured data and for identifying possible out-of-plane eccentricities that might be present during testing.

The geometry and instrumentation of the specimen is shown in figure 1. This specimen was made from high modulus graphite-fiber epoxy resin composite (Modnor I/epoxy (MOD I/E)). The laminate configuration of the specimen con-

sisted of 8-plies $[0_8]$, all oriented in the same direction. The specimen thickness was about .057 inch and it was loaded at 30° to the fiber direction.

The NASTRAN model is shown in figure 2. The NASTRAN model consisted of 657 nodes and 576 quadralateral plate (CQUAD2) elements which included the tapered portion of the reinforcing end tabs. Note that the finite element representation includes two groups of elements. At each end, the elements are 0.0625 in. long; these represent the tapered portion of the reinforcing tabs and the first quarter inch segment of the test section which is the site of the top strain gages. The remaining elements of the representation are 0.125 inch in length. All elements for this model are 0.0625 wide. The element size was made small enough to study the zones where the strain gages were located on the actual specimen. The material properties required for NASTRAN were generated using the composite mechanics code (ref. 1). Typical CPU (central processing unit) time was 18 minutes for the UNIVAC 1110.

Axial strains across the width of the 30° off-axis specimen as determined by NASTRAN are shown in figure 3 along with the measured fracture strains. Midlength measured strains at fracture ranged from 0.365 to 0.380 percent while those at the tab end were 0.395 and 0.424 percent. The NASTRAN analysis axial strains across the specimen midlength were between 0.374 and 0.426 percent and those at the tab-end were between 0.353 and 0.447 percent. A glance of figure 3 shows that NASTRAN predicted strains are a little higher than the measured strains at the specimen midlength and lower than the measured strains near the specimen end. Although not shown in figure 3, NASTRAN strain predictions for a section of the specimen lying midway between the tab-end and specimen midlength were between the two curves, as would be expected. The discrepancy between the strains measured at midlength and tab-end of the specimens are not accounted for by the NASTRAN analysis.

This leads to the conclusion that the discrepancy is probably produced by possible out-of-plane load eccentricities which were investigated and are described in the next section. The important point to be noted is the use of NASTRAN in identifying possible test difficulties.

OUT-OF-PLANE ECCENTRICITIES IN COMPOSITE OFF-AXIS SPECIMENS

The objective of using NASTRAN in this study was to assess whether possible out-of-plane of the specimen eccentricities such as bending or twisting could produce part or all of the discrepancy described in the previous section.

The geometry of the specimen and the NASTRAN model are the same as described in the previous section (figs. 1 and 2, respectively). For this study, the specimen was first loaded with an out-of-plane (plane of specimen) bending moment and then with a twisting moment at one end of the specimen. The ends of the specimen were constrained to lie in the same plane for the out-of-plane bending case. The center line of the specimen was constrained to lie in the same plane for the twisting case.

The out-of-plane bending effects predicted by NASTRAN on axial strain for the 30° off-axis specimen subjected to a 100 inch-pound bending moment are

shown in figure 4. Those for torsion are shown in figure 5 (100 in.-lb twisting moment).

At specimen midlength, the twisting effects are very small, figure 5, but near the grip they are important and are of opposite signs on the two edges of the specimen. The out-of-plane bending effects shown in figure 4 are moderate but all in the same direction at specimen midlength. Near the tab they are of the opposite sign and are much larger at one edge of the specimen than at the other. The combined effect of twisting and out-of-plane bending near the tab end of the tensile specimen could be sizeable and data provided by a strain gage at such a location could be erroneously interpreted.

The important conclusion from the previous discussion is: out-of-plane eccentricities of tensile specimens could give rise to very large strains near the end tabs of the specimen. This may be a cause of the frequent failure of this type specimen near the tab. It is significant to note that to have arrived at the same interpretation through the use of strain gages would have required a large number of strain gages which would have been impractical. Therefore, the effectiveness of using NASTRAN in this study as a research tool is obvious.

VIBRATION OF COMPOSITE SPECIMENS WITH DEFECTS

The objective of using NASTRAN in this study was to predict the effects of defects in composite specimens on the free vibration modes of these specimens. For this purpose, the vibration modes of composite specimens with progressively larger through-the-thickness defects were determined.

The specimen geometry is shown in figure 6. The specimen analyzed was assumed to be made from Thornell 75/Epoxy (T75/E)$[\pm 45, 90, 90, 0, 0]_s$ composite. The defects considered were slits 1/4, 1/2, and 3/4 of the specimen width, in length, respectively, and 1/4 inch wide.

The NASTRAN model is shown in figure 7. The model consists of 297 nodes and 256 CQUAD2 elements. The through-the-thickness defect was simulated by removing elements 124 and 125 for the 1/4, 123 to 126 for the 1/2, and 122 to 127 for the 3/4 size defect, respectively. The material properties required for NASTRAN were obtained from the composite mechanics computer code (ref. 1). Typical CPU times were 17 minutes in the UNIVAC 1110.

Free vibrational frequencies were calculated for an undamaged specimen and for a specimen with defects at midlength which spanned 1/4, 1/2, and 3/4 of the width of the specimen by removing the connection cards for the appropriate elements. Table I shows the frequencies for the first four modes for each condition. The frequencies are lowered by the defect. Table II shows the percent reduction in specimen area resulting from the defects of the three sizes as well as the relative changes in the corresponding frequencies. A defect spanning one-fourth of the specimen width which removes 0.78 percent of the bulk of the material in the specimen reduces the vibrational frequency by no more than 1.2 percent in the case of the first four modes. This would represent a very large crack in an actual component, which leads to the conclusion that it would take a large defect or imperfection to affect the integrated stiffness and mass of

the component. Also the vibration frequencies are not very sensitive to small defects in composite structures. Figure 8 shows the fourth mode shapes for an undamaged composite specimen and the 1/2 size defect (1.56 percent of the specimen area). The mode shapes are almost identical and the frequency drop due to this large defect is less than 3.0 percent.

The important conclusion from this study is that the vibration frequency measurement used as an NDE procedure for evaluating a composite structure with defects of the type investigated is not likely to prove a practical procedure. This example illustrates the use of NASTRAN as a research analysis tool for assessing the practicality of such NDE procedures.

TRANSITION REGION STRESSES IN TUBULAR COMPOSITE SPECIMENS

The objective of using NASTRAN in this study was to predict the stress state near the grip area (transition region) in thin composite tubular specimens. The predicted stress state was used to (1) compare it with measured data and (2) more importantly, evolve grip designs which minimize the stress in the transition region. Thin tubular specimens are important in studying failure and failure mechanisms of composites subjected to controlled combinations of multiaxial loading, references 2 and 3.

Numerous grip failures were occurring in tests of tubular unidirectional composite test specimens. The specimens were potted into metal grips with an epoxy resin as shown in figure 9. One of these specimens was instrumented with strain gages in the grip transition region so that predicted results using NASTRAN could be compared with measured data. The geometry of the specimen which was used in the NASTRAN stress analysis is shown in figure 10. The composite material used in the analysis was MOD I/E with a laminate configuration of $[0_8]$. The material properties required for use in NASTRAN were determined from data provided by the material supplier.

A schematic of the NASTRAN model is shown in figure 11. The model consisted of 576 nodes and 552 CQUAD2 elements, 24 around the circumference and 23 along the length. These elements were used to model the tube wall and the potting material. The elements representing the potting material were normal to those for the tube wall. Typical computer CPU times were 21 minutes in the UNIVAC 1106.

Figure 12 compares the experimental and predicted results. The good agreement between the predicted results and the experimental data gave confidence in the NASTRAN model. It was then used to determine the effect on grip transition stresses of different grip designs and potting material properties. With the aid of this model it is possible to identify grip designs with reduced transition stresses and, thereby, evolve a more practical grip design.

BENDING MODULUS OF COMPOSITE ANGLEPLIED LAMINATES WITH SOME THICKNESS VARIATION

The objective of using NASTRAN in this study was to identify an effective

means for determining the bending modulus of specimens from composite angleplied laminates with variations in thickness. The bending modulus and the usual elastic modulus, measured in a tensile test, are different for angleplied laminates in general.

The material was MOD I/E and was in the form of tensile specimens with end tabs already in place and the thickness of the test section varied by as much as 7 percent. For cantilever bending, stiffness is related to fundamental frequency by the following expression:

$$E = 3.2\, f_1^2 \frac{\bar{m} L^4}{I} \tag{1}$$

where E is the bending modulus, f_1 is the fundamental frequency, $\bar{m}$ is the mass per unit length, L is the length of the cantilever, and I is the moment of inertia.

The fundamental frequency was determined experimentally. To relate this frequency to bending modulus, the specimen was modeled for NASTRAN taking into account the thickness variation and the end tab. Assuming that the bending modulus was constant along the length of the specimen, the modulus was determined from the relationship

$$E_e = E_N \left(\frac{f_e}{f_N} \right)^2 \tag{2}$$

where E_e is the effective bending modulus, E_N is a trial bending modulus used in the NASTRAN model, f_e is the experimentally determined fundamental bending frequency, and f_N is the fundamental frequency obtained from the NASTRAN model. Schematics of the tensile specimen and the NASTRAN model are shown in figure 13. Bending moduli determined from the above procedure for four quasi-isotropic angleplied laminates with different laminate configurations are shown in table III. This example illustrates the versatility of NASTRAN.

HIGH VELOCITY IMPACT COMPOSITE CANTILEVER SPECIMENS

The objective of the NASTRAN stress analysis of this specimen was to determine high stress regions and stress types under point load. The information obtained was used to: (1) guide the selection of sites for placing strain gages to measure the high velocity impact response of composite centilevers and (2) to help interpret some of the high velocity impact data generated in reference 4 under contract to NASA LeRC.

A photograph of an impacted specimen reported in reference 4 is shown in figure 14. The geometry of the specimen is depicted in figure 15. The NASTRAN model is shown in figure 16. The NASTRAN model consisted of 333 nodes and 288 CQUAD2 elements. Typical CPU times were about 4.5 minutes in the UNIVAC 1110. The specimen, for which results will be presented, was made from intraply hybrid composite with the following constituents: 75-percent type AS graphite fiber-epoxy resin composite (AS/E) and 25-percent S-glass - epoxy resin com-

posite (S-G1/E). The laminate configuration for the specimen was $[\pm 40, 0, 10, 0, -10]_2$ which is representative of composite blade airfoil laminate configurations to minimize residual stresses. The material properties required for use in NASTRAN were generated using the composite mechanics code, ref. 1.

Predicted stresses on the back surface of the composite specimen due to a unit point load at the impact point are shown in stress contour plots as follows (refer to fig. 16 for directions): spanwise stress (σ_x) in figure 17(a), chordwise stress (σ_y) in figure 17(b), and in-plane shear stress (σ_{xy}) in figure 17(c). The important points to be observed from these stress contour plots are:

1. High spanwise stresses at the support near the specimen center, figure 17(a)
2. High chordwise stresses near the specimen center, in-board from the impact point, figure 17(b)
3. High in-plane shear stresses at the specimen edges near the support, figure 17(c)

The important conclusion from the above observations is that high stress regions for these types of specimens are readily identified using NASTRAN. Strain gages should be placed at these regions for obtaining optimum information. It is also important to note that the estimated maximum impact force built up during these tests is about 1000 pounds for 700 feet per second projectile velocity within 50 microseconds from initial contact (ref. 5). This magnitude of impact force will produce high tensile chordwise stresses in the back surface of the specimen near the impact point, figure 17(b), which, in turn, will produce splitting and delaminations at this region. This is consistent with the test result exhibited in figure 14.

HIGH-TIP-SPEED COMPOSITE FAN BLADE

The original objective of this investigation was to develop a computerized capability which couples NASTRAN with composite mechanics for the structural and stress analysis of composite fan blades for aircraft engines. A description of this capability and results obtained therefrom have been reported previously in references 6, 7, and 8. Herein, predicted stresses at design loads are compared with fracture stresses in tensile specimens cut from the critically stressed region in the composite blade. The design loads include aerodynamic pressure and temperature, and centrifugal forces resulting from 2200 feet per second tip speed with a mean tip radius of 16.4 inches (ref. 6).

A photograph of the fabricated composite blade is shown in figure 18. The blade is twisted, cambered, and tapered (both spanwise and chordwise). The blade was made from high-tensile-strength graphite fiber in Kerimid polyimide matrix (HTS/K601). The blade consisted (blade laminate configuration) of 73 plies at its thickest portion 30-percent of which were oriented at $\pm 40^\circ$ to the radial direction at the surface (shell plies) and 70-percent were oriented at 0° to the radial direction at the center (core plies). This type of laminate configuration is usually called shell/core. In addition, the blade had $\pm 20^\circ$ transition plies between the $\pm 40^\circ$ shell plies and the 0° core plies, and also $\pm 70^\circ$ plies near the tip for increased flutter resistance. For additional de-

tailed description see references 6 and 8.

The NASTRAN model of the composite blade is shown in figure 19. The model consisted of 299 nodes and 531 triangular plate (CTRIA2) elements. Typical CPU times were 11.5 minutes in the UNIVAC 1106. The average stresses predicted by NASTRAN for the design load are shown in a contour plot in figure 20. Stresses from the high stress region points A, B, and C in figure 20 are tabulated in table IV. Also shown in this table are the material fracture stresses measured using tensile specimens cut from the same region from fabricated blades (in situ material fracture stresses). As can be seen in table IV, the predicted stresses on the pressure surface are higher than the fracture stress. As a point of interest, some of these blades failed below or at design load during spin tests.

The important conclusion from the previous discussion is that NASTRAN coupled with composite mechanics can be used to predict fracture stress in structural components with complex geometry in anisotropic heterogeneous materials. The significant point to be emphasized here is that predicted stresses must be compared with in situ material fracture stresses for reliable assessment of the design.

FIBER COMPOSITE THIN SHELL AIRFOIL

The objective of this study was to select on a preliminary design basis a laminate configuration for NACA 64A010 type airfoils for wind tunnel wing simulation studies. The design load conditions were: (1) dynamic pressure typical for this type of airfoil, (2) first mode natural frequency of 60 Hz or greater, and (3) a maximum weight of 20 pounds. The margin of safety on stresses due to dynamic pressure was about 5, to account for possible fatigue, and on the first mode frequency was about 1.5.

The geometry of the airfoil section is shown in figure 21. Note the airfoil is a thin shell so that the weight is kept to a minimum. The composite material selected was graphite/epoxy (AS/E) 32 plies (0.005 in./ply) for a laminate thickness of 0.160 inch. The laminate configuration was $[(\pm 45)_2, 90_2, 0_{10}]_s$. The density of the composite is about 0.054 pound per inch^3 resulting in an airfoil weight of 18 pounds which is 2 pounds less than the design requirement. The NASTRAN model is shown in figure 22 (a-suction surface and b-pressure surface) and consisted of 130 nodes and 120 CQUAD2 elements. The material properties required for use in NASTRAN were generated using the composite mechanics code (ref. 1). Typical CPU time for the UNIVAC 1110 was: 7 minutes for the static case and 15 minutes for the first 10 vibration modes.

NASTRAN predicted spanwise stresses on the suction surface are shown in stress contour plots in figure 23(a), and for the pressure surface in figure 23(b). The maximum bending stress predicted by NASTRAN was about 7 ksi in the spanwise direction near the 1/3 chord point at midspan. The corresponding fracture stress measured in laboratory specimens with the same laminate configuration was 128 ksi which is much more than five times the design load stress of 7 ksi. Analogous comparisons were found for the other stresses.

The first eight vibration modes predicted by NASTRAN are tabulated in ta-

ble V where the predominant vibration mode shape is also identified. The first predicted mode is 90 Hz which is 1.5 times the minimum design requirement of 60 Hz. An interesting result from the vibration analysis is the second mode which is an accordion type mode shape.

It is important to note that the laminate configuration described above was arrived at after two NASTRAN analysis cycles. This laminate configuration is not claimed to be optimum. Nevertheless, the example illustrates convincingly the effectiveness of NASTRAN as an analysis tool in the preliminary designs of composite airfoils.

SUMMARY OF RESULTS AND CONCLUSIONS

The major results and conclusions of this investigation are as follows:

1. Out-of-plane eccentricities such as bending and twisting give rise to very large strains near the tab ends of off-axis composite tensile specimens and thereby initiate fracture at these locations.
2. Vibration frequency measurements for evaluating the presence and/or effects of small defects (about 2 percent by volume) in composites may not prove practical.
3. Grip and/or end attachments can be designed to minimize transitional region strains due to load transfer in thin composite tubes using NASTRAN with plate elements.
4. Effective bending moduli of composites with variable thickness can be determined using NASTRAN in conjunction with suitable frequency measurement experiments.
5. NASTRAN can be used to help establish an effective plan for instrumenting high-velocity-impact composite specimens.
6. Stresses predicted using NASTRAN must be compared with in-situ material fracture stresses for reliable assessment of the design.
7. The number of iteration analysis cycles in sizing airfoil-type composite components may be kept to as small as two with judicious use of NASTRAN.
8. The results of the various analyses described in this summary paper demonstrate rather convincingly the versatility and effectiveness of NASTRAN as an analysis research tool in the rapidly advancing methodology associated with composite mechanics and composite structural components.

REFERENCES

1. Chamis, Christo C.: Computer Code for the Analysis of Multilayered Fiber-Composites: User's Manual. NASA TN D-7013, 1971.

2. Sullivan, T. L.; and Chamis, C. C.: Some Important Aspects in Testing High-Modulus Fiber Composite Tubes Designed for Multiaxial Loading. NASA TM X-68045, 1972.

3. Chamis, C. C.; and Sullivan, T. L.: Combined-Load Stress-Strain Relationships for Advanced Fiber Composites. NASA TM X-71825, 1976.

4. Pike, R. A.; and Novak, R. C.: Design, Fabrication and Tests of Multi-Fiber Laminates. (R75-911730-15, United Aircraft Corp.; NAS3-17778), NASA CR-134763, 1975.

5. Friedrich, L. A.; and Preston, J. L., Jr.: Impact Resistance of Fiber Composite Blades Used in Aircraft Turbine Engines. (PWA-TM-4727, Pratt and Whitney Aircraft; NAS3-15568), NASA CR-134502, 1973.

6. Chamis, C. C.; and Lynch, J. E.: High-Tip-Speed Fiber Composite Fan Blades: Vibration and Stress Analysis. NASA TM X-71589, 1974.

7. Chamis, C. C.; and Minich, M. D.: Structural Response of a Fiber Composite Compressor Fan Blade Airfoil. NASA TM X-71623, 1975.

8. Chamis, C. C.: Vibration Characteristics of Composite Fan Blades and Comparison with Measured Data. 17th Conference on Structures, Structural Dynamics, and Materials. Am. Inst. Aeron. Astron., Inc., 1976, pp. 98-104.

TABLE I. - FREE VIBRATION FREQUENCIES OF GRAPHITE/EPOXY (THORNEL 75/epoxy $[\pm 45, 90_2, 0_2]_s$) COMPOSITE LAMINATE WITH DEFECTS

Defect ratio $\left(\frac{a}{w}\right)$	Frequency (Hz) for Mode			
	1	2	3	4
0	1385.9	3907.0	5453.9	7819.4
1/4	1368.9	3906.6	5399.3	7763.4
1/2	1321.5	3903.5	5345.0	7589.1
3/4	1215.8	3895.1	5282.4	7261.9

a = defect width
w = specimen width

TABLE II. - CHANGE IN FREE VIBRATION FREQUENCIES CAUSED BY DEFECTS (THORNEL 75/EPOXY $[\pm 45, 90_2, 0_2]_s$)

Length of defect $\left(\frac{a}{w}\right)$	Defect area (percent of total area)	Percent change in frequency for mode shown			
		1	2	3	4
1/4	0.781	-1.2	-0.01	-1.0	-0.7
1/2	1.56	-4.6	-0.09	2.0	-2.9
3/4	2.34	-12.3	-0.3	3.1	-7.1

a = defect width
w = spedimen width

TABLE III. - SUMMARY OF BENDING MODULI OF QUASI-ISOTROPIC COMPOSITES FROM GRAPHITE/EPOXY (MODMOR I/ERLA 4617)

Layup	Outer fiber direction	Bending modulus* (10^6 psi)
$(0, \pm 60)_s$	0	21.2
	90	3.4
$(0, \pm 45, 90)_s$	0	16.4
	90	3.4
$(0, \pm 30, \pm 60, 90)_s$	0	17.6
	90	3.0
$(0, \pm 22.5, \pm 45, \pm 67.5, 90)_s$	0	17.2
	90	2.8

*Average of two tests.

TABLE IV. - COMPARISON OF COMPUTED AND FRACTURE STRESSES AT REGION OF MAXIMUM AVERAGE COMPOSITE STRESS AT DESIGN LOAD

Blade point schematic	Surface stresses, ksi	
	Computed	Fracture[a]
A(S.S.)[b]	-7.86	52.3 - 65.4
(P.S.)	67.1	
B(S.S.)	-6.18	
(P.S.)	64.16	
C(S.S.)	-4.75	
(P.S.)	66.0	

[a]Measured in tensile specimens cut from fabricated blade.

[b]For location of these points, see fig. 20; S.S. denotes suction surface; P.S. denotes pressure surface.

TABLE V. - NASTRAN VIBRATION RESULTS FOR A FIBER

COMPOSITE THIN SHELL AIRFOIL

Mode number	Frequency, Hz	Predominant mode shape
1	90	First spanwise bending (1SB)
2	118	Accordian type
3	135	Coupled torsion-bending (TB)
4	157	Coupled spanwise-chordwise bending
5	181	First torsion (1T)
6	187	Second torsion (2T)
7	229	Third torsion (3T)
8	245	Second chordwise bending (2CB)

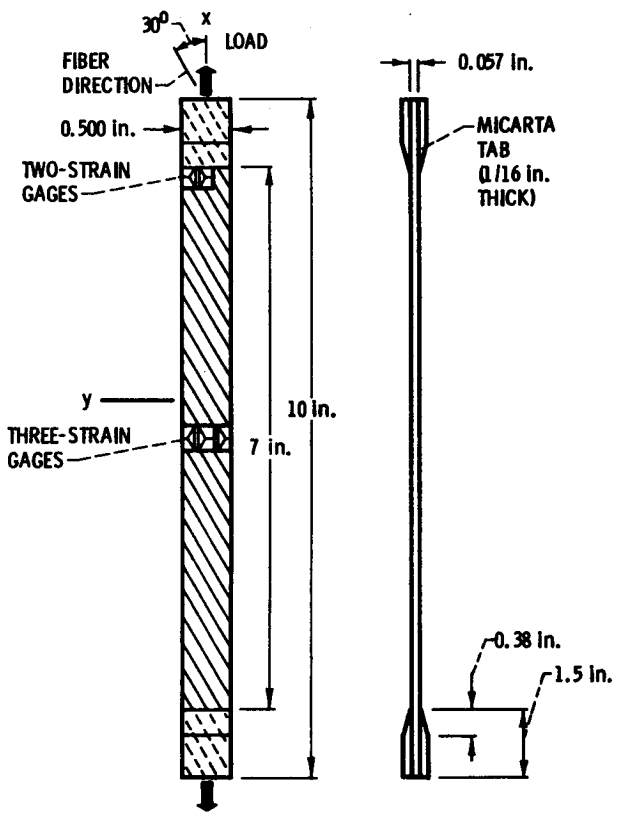

Figure 1. - Specimen geometry and instrumentation of off-axis specimen ($[0_8]$ MOD I/E).

Figure 2. - NASTRAN model of off-axis specimen (657 nodes; 576 CQUAD2 elements).

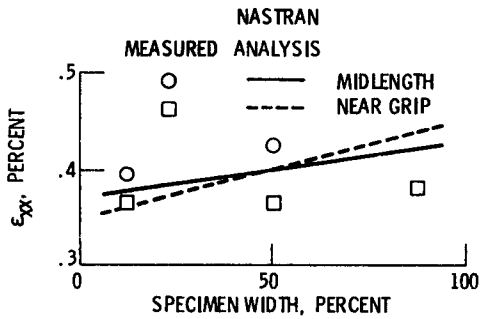

Figure 3. - Axial strain variation across 30^0 off-axis tensile specimen of graphite/epoxy composite (MOD I/E $[0_8]$).

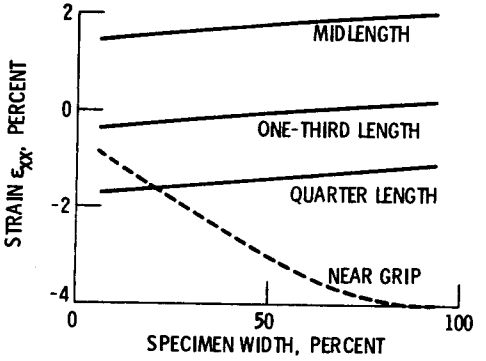

Figure 4. - Out-of-plane bending effects on axial strain of the 30^0 off-axis specimen (100 in.-lb bending moment).

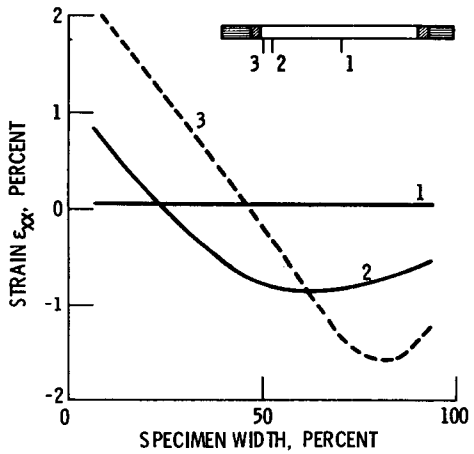

Figure 5. - Twisting effects on axial strain of the 30^0 off-axis specimen (100 in.-lb torque).

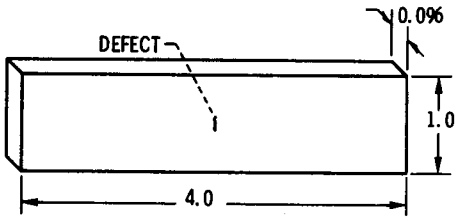

Figure 6. - Schematic of specimen with defects (T-75/PR288 $[45, -45, 90, 90, 0, 0]_S$, all dimensions are in inches).

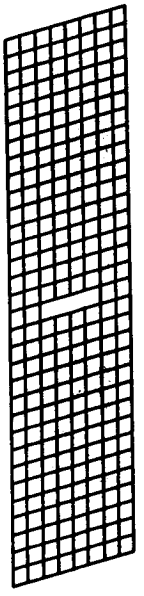

Figure 7. - NASTRAN model for composite specimens with defects; (297 nodes; 256 elements).

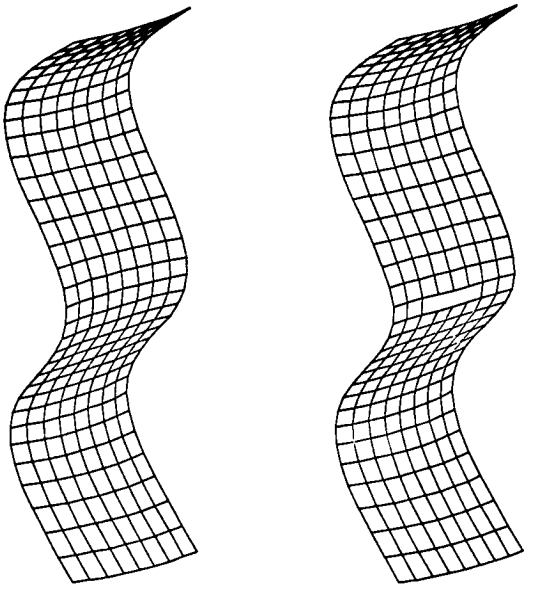

(a) NO DEFECT FREQUENCY: 7819 Hz.

(b) WITH DEFECT (a/w = 1/2) FREQUENCY: 7589 Hz.

Figure 8. - Fourth free vibration mode shape of composite specimen with and without defect.

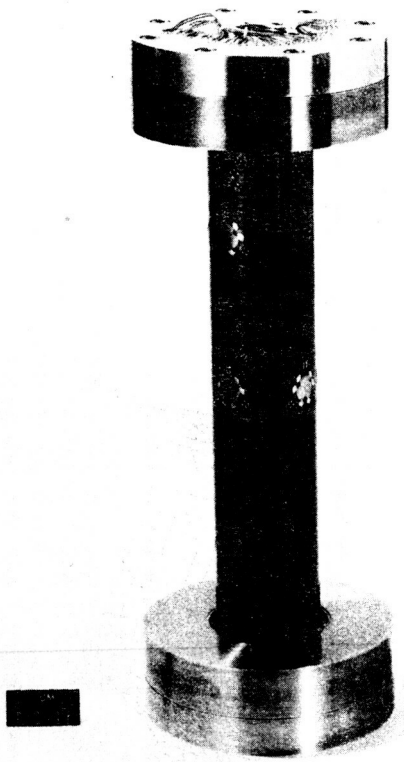

Figure 9. - Photograph of instrumented tube mounted in grips, (MOD I/E, $[0_8]$).

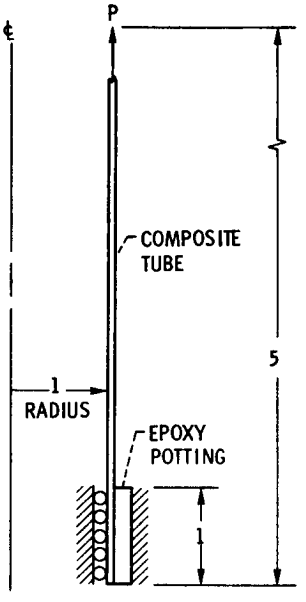

Figure 10. - Schematic of thin composite tubular specimen. (All dimensions are in inches.)

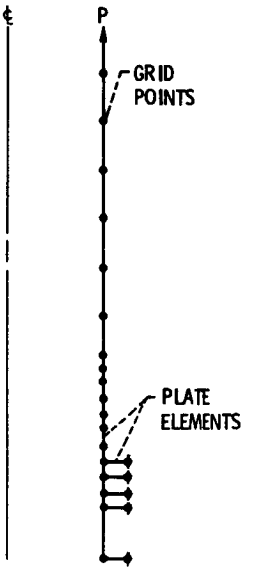

Figure 11. - Schematic of NASTRAN model (Quadrilateral plate elements).

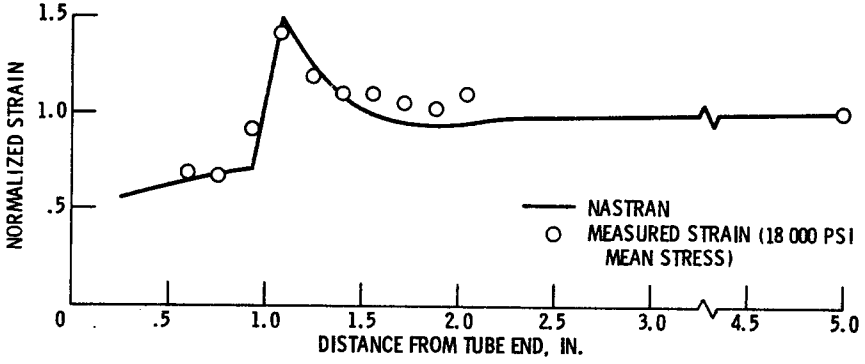

Figure 12. - Comparison of predicted and measured strains for a unidirectional composite tube.

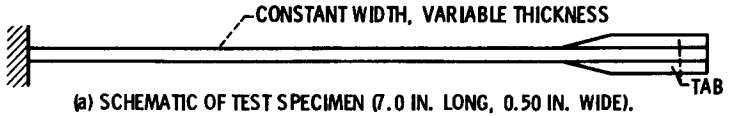

(a) SCHEMATIC OF TEST SPECIMEN (7.0 IN. LONG, 0.50 IN. WIDE).

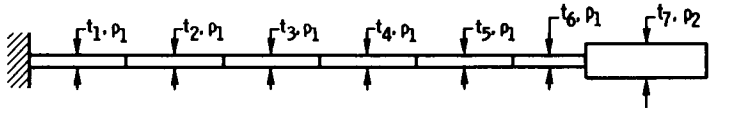

(b) SCHEMATIC OF NASTRAN MODEL (BAR ELEMENTS).

Figure 13. - Geometry and NASTRAN model for a composite angleplied laminate (t = thickness, ρ = density).

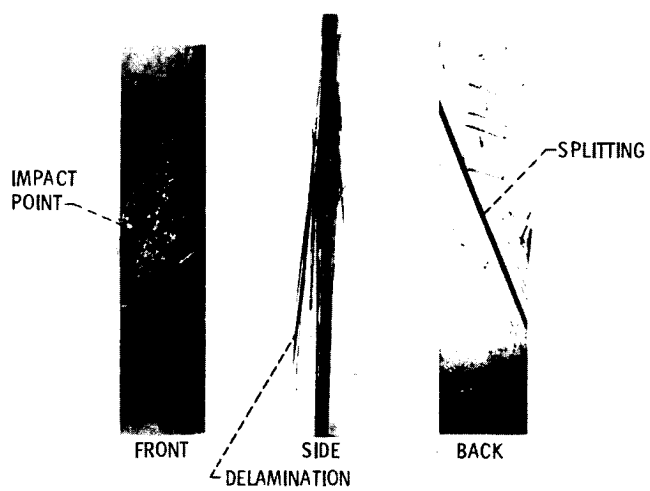

Figure 14. - Typical composite cantilever specimen after high velocity impact test (ref. 4).

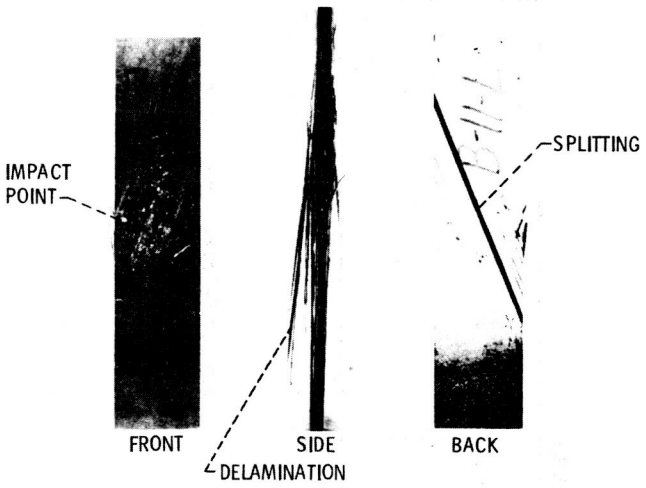

Figure 14. - Typical composite cantilever specimen after high velocity impact test (ref. 4).

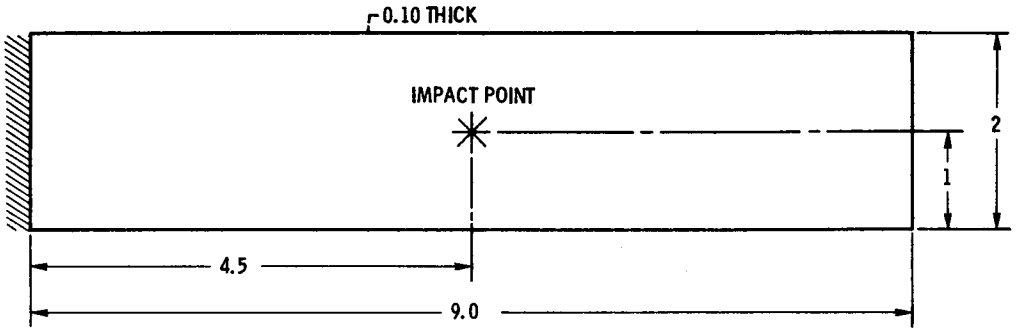

Figure 15. - Geometry of composite cantilever specimen for high velocity impact studies. (Dimensions are in inches.)

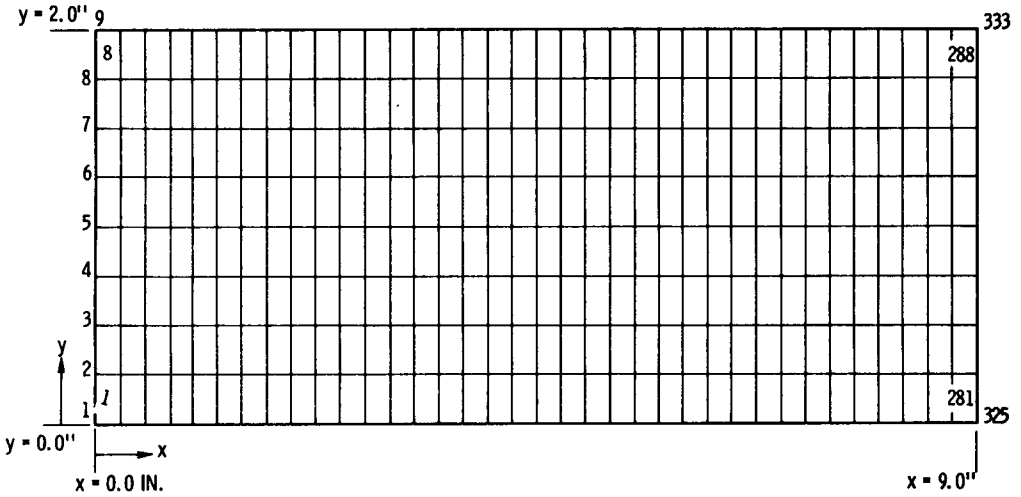

Figure 16. - NASTRAN model of the composite cantilever impact specimen (333 nodes; 288 CQUAD2 elements).

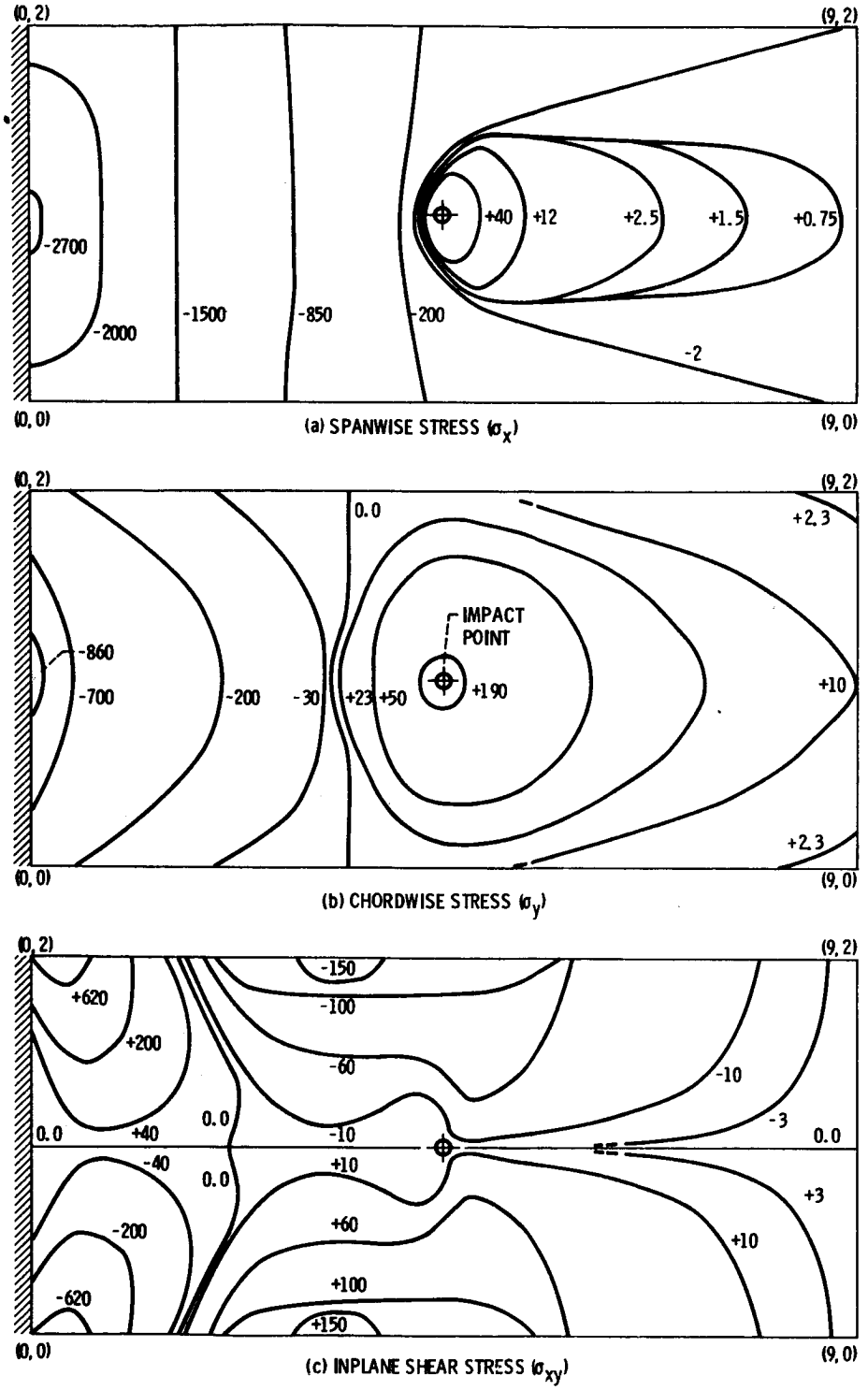

Figure 17. - NASTRAN predicted stress contours due to unit load at impact point (AS/S-Glintraply hybrid $[\pm 40, 0, 10, 0, -10]_s$).

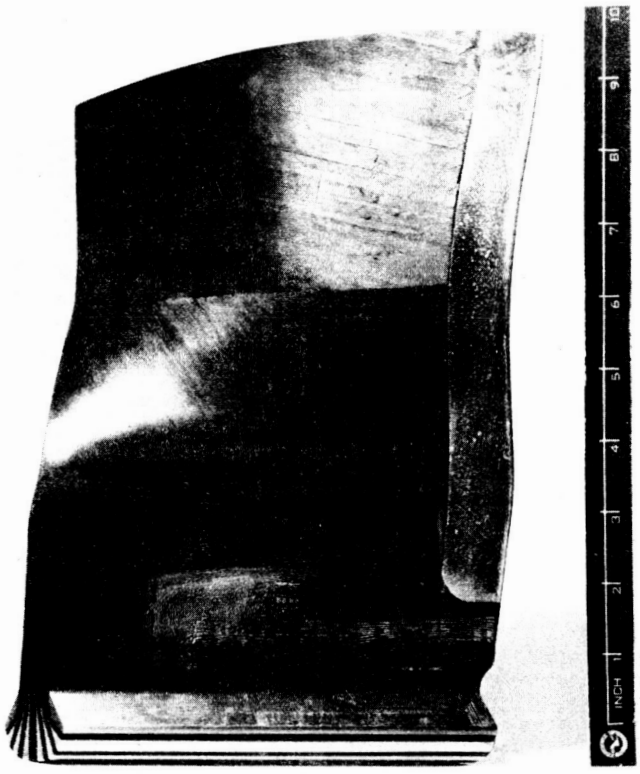

CS-76354

Figure 18. - Photograph of high-tip-speed composite blade. HTS/K601, (±40, ±20, 0).

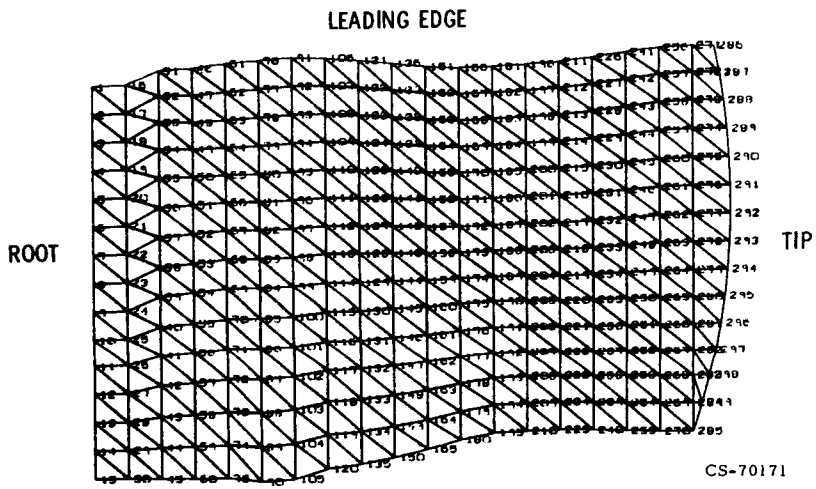

Figure 19. - NASTRAN finite element representation for fiber composite blade.

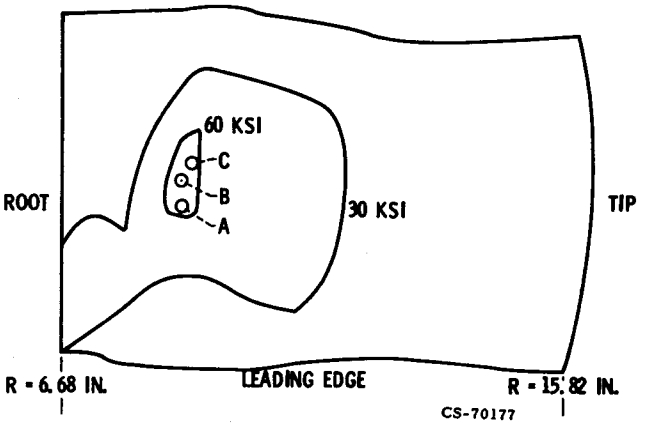

Figure 20. - Predicted average composite radial stress contours on pressure surface.

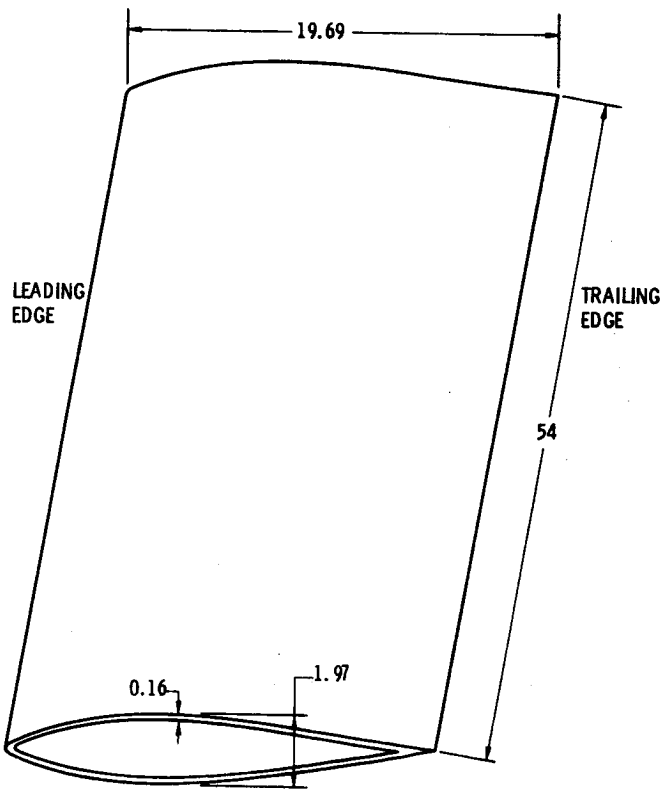

Figure 21. - Schematic of airfoil geometry (NACA 64A010; Dimensions in inches; laminate AS/E; $[(\pm 45)_2, 90_2, 0_{10}]_s$; attack angle $\approx 15^0$).

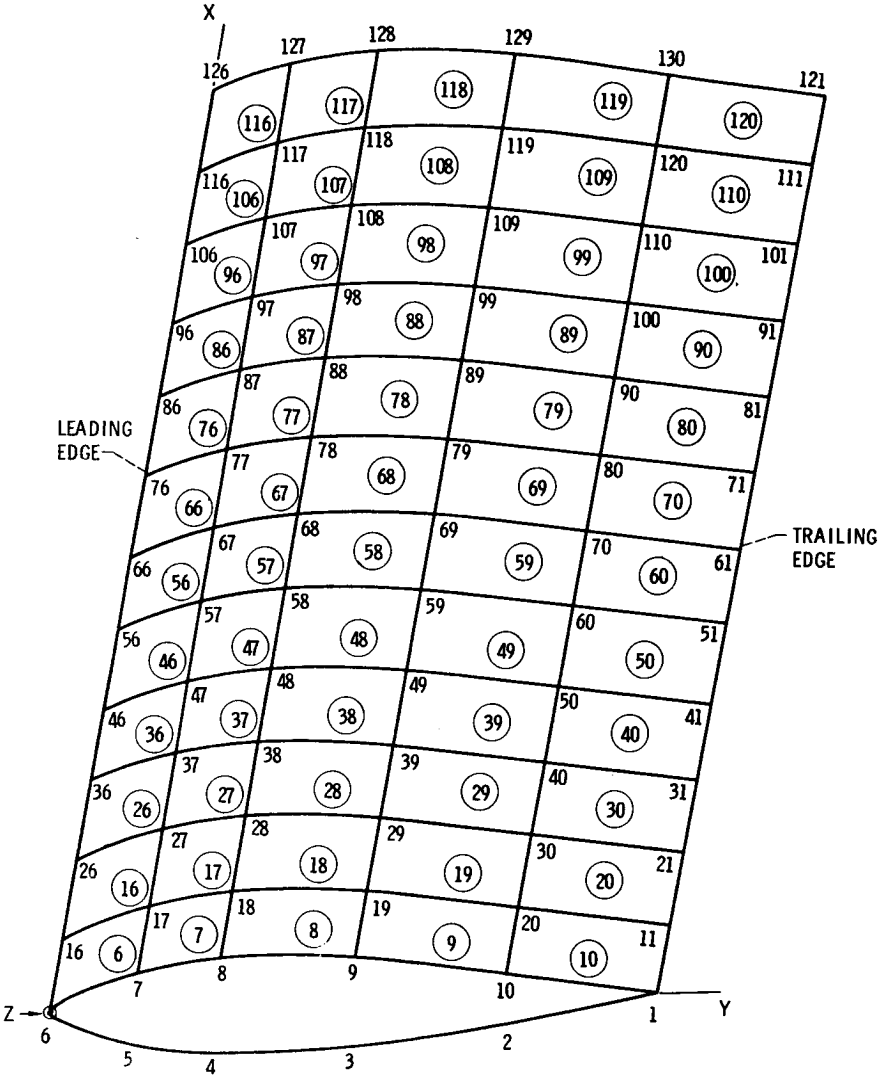

(a) SUCTION SURFACE.

Figure 22. - Airfoil NASTRAN model (130 nodes; 120 CQUAD2 elements).

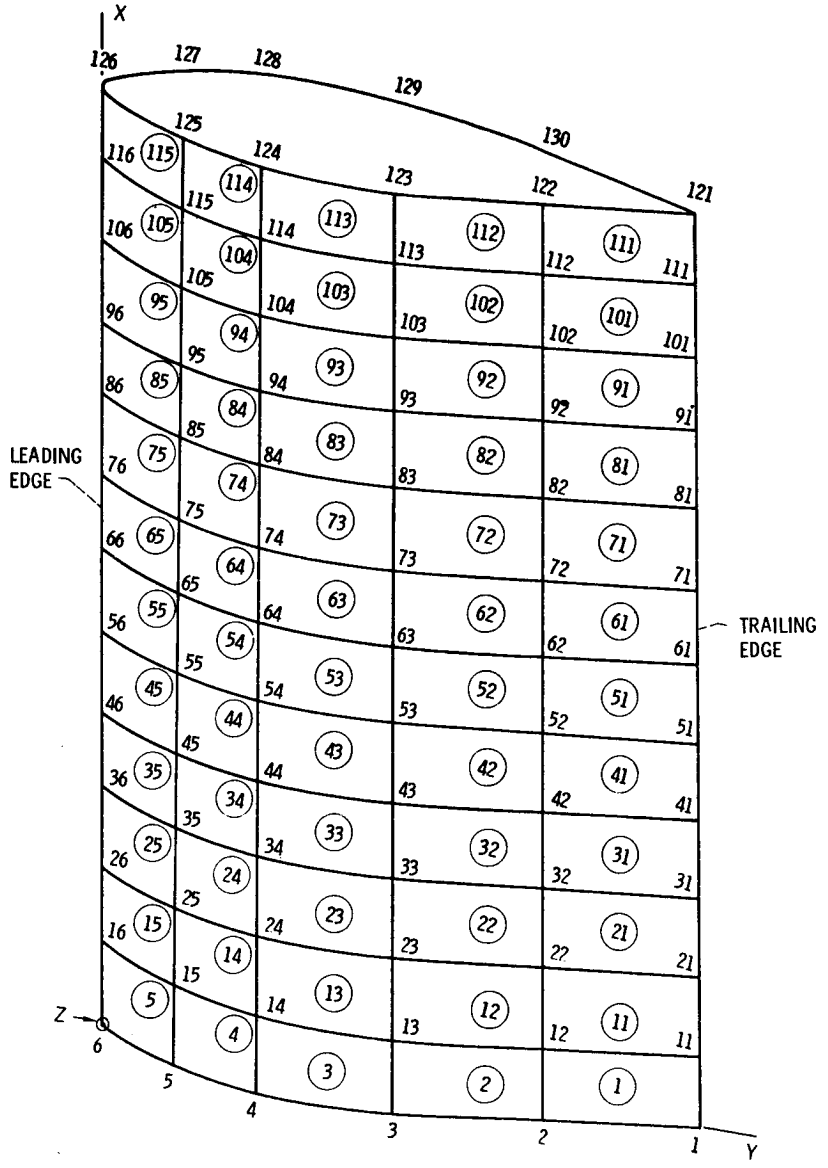

(b) PRESSURE SURFACE

Figure 22. - Concluded.

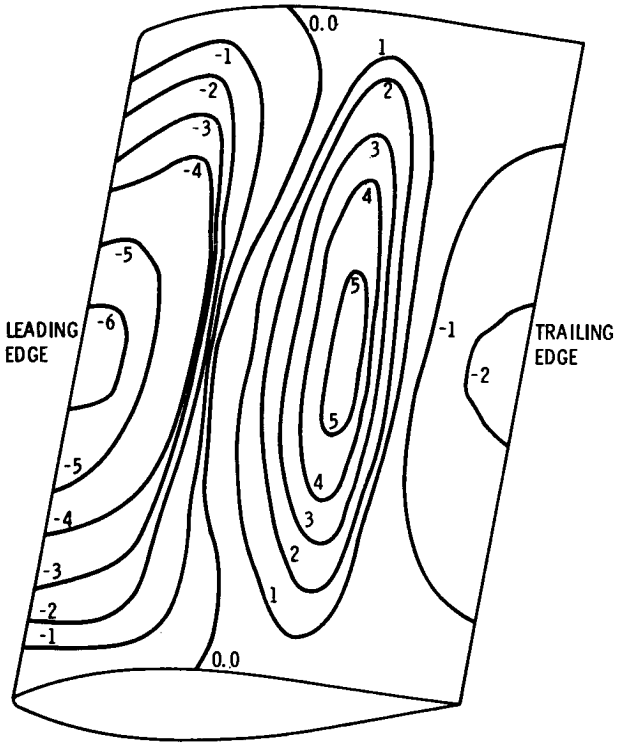

(a) SUCTION SIDE.

Figure 23. - NASTRAN predicted stress contour plots (ksi) in the spanwise direction on the outer surface of a composite airfoil (NACA 64A010).

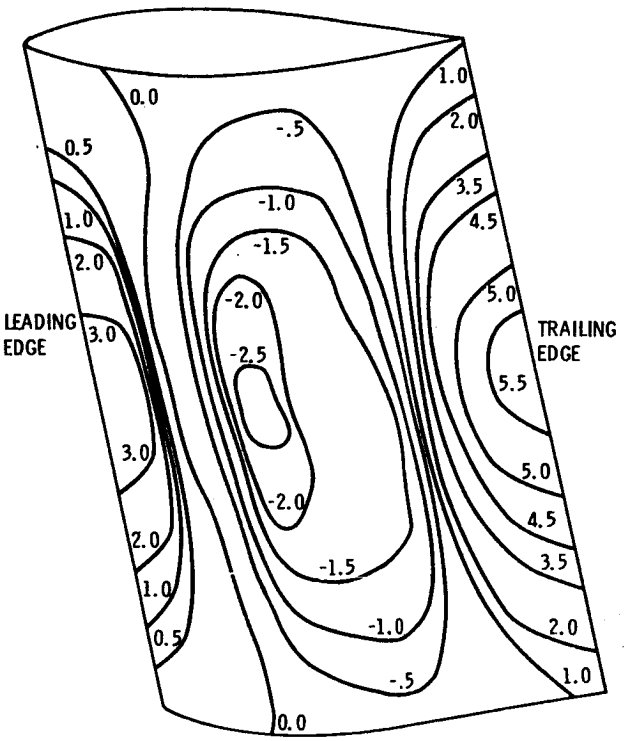

(b) PRESSURE SIDE.

Figure 23. - Concluded.